JOURNAL OF MATERIALS PROCESSING TECHNOLOGY 196 (2008) 190–196

journal homepage: www.elsevier.com/locate/jmatprotec

Application of BPANN for prediction of backward ball spinning of thin-walled tubular part with longitudinal inner ribs

Shuyong Jiang[a,*], *Zhengyi Ren*[a], *Kemin Xue*[b], *Chunfeng Li*[c]

[a] *Engineering Training Center, Harbin Engineering University, Harbin 150001, PR China*
[b] *School of Materials Science and Engineering, Hefei University of Technology, Hefei 230000, PR China*
[c] *School of Materials Science and Engineering, Harbin Institute of Technology, Harbin 150001, PR China*

ARTICLE INFO

Article history:
Received 31 October 2006
Received in revised form
24 April 2007
Accepted 17 May 2007

Keywords:
Power spinning
Ball spinning
Artificial neural networks
Longitudinal inner ribs
Back-propagation algorithm

ABSTRACT

As a successively and locally plastic deformation process, backward ball spinning is applied for the purpose of manufacturing thin-walled tubular part with longitudinal inner ribs. Obtaining the desired inner ribs is one of the most critical tasks in backward ball spinning of thin-walled tubular part with longitudinal inner ribs and the formability of inner ribs depends greatly on the process parameters, such as ball diameter, feed ratio, wall thickness reduction and wall thickness of tubular blank. As a nonlinear dynamics system simulating structure and function of biological neural network in the human brain, back-propagation artificial neural network (BPANN) is used in backward ball spinning of thin-walled tubular part with longitudinal inner ribs. The attractiveness of BPANN comes from its remarkable information processing characteristics pertinent mainly to nonlinearity, adaptability, high parallelism, learning capability, fault and noise tolerance so that it can be more efficient in solving complex and nonlinear optimization problems in backward ball spinning of thin-walled tubular parts with longitudinal inner ribs. Not only can BPANN successfully predict the formability of the inner ribs, but it can simulate the influences of the process parameters on the height of inner ribs as well. In the end, the process parameters are matched so rationally that the desired spun parts can be obtained.

1. Introduction

Tube spinning, also known as tube flow forming or tube power spinning, is a typically successively and locally plastic deformation process, which is used to produce a hollow shape product with a surface of revolution by transforming a thick-walled preform into a long and thin-walled workpiece (Wong et al., 2003). Tube spinning not only needs low load capacity and low production cost, but also manufactures components with high mechanical properties and smooth surface finish by means of less complex tooling (Chang et al., 1998; Xue and Lu, 1997).

Ball spinning belongs to tube spinning using balls as deformation tool instead of rollers (Rotarescu, 1995). Ball spinning process is characterized by its fairly small deformation zone and its relatively low forming loads as compared with tube spinning using rollers. Furthermore, stress of deformation zone in the process is so high as to be easy to meet yield criterion. Especially as for backward ball spinning process, the metal of deformation zone is caused to be in a three-

* *Corresponding author*. Tel.: +86 451 82519952; fax: +86 451 82519952.
E-mail address: jiangshy@sina.com (S. Jiang).
0924-0136/$ – see front matter © 2007 Elsevier B.V. All rights reserved.
doi:10.1016/j.jmatprotec.2007.05.034

dimension compressive stress state so that it has a good plasticity. In addition, balls are distributed so uniformly along the circumference of deformation zone that the circumferential flow of metal of deformation zone is confined so as to make the mandrel keep good balance and stability. Based on the advantages mentioned above, ball spinning has been the best process to form thin-walled tubular parts with high strength, high precision, and good surface quality (Jiang et al., 2004, 2006).

In the paper, backward ball spinning is used for forming thin-walled tubular parts with longitudinal inner ribs, which is a relatively new attempt. Mechanism of backward ball spinning of thin-walled tubular parts with longitudinal inner ribs is pretty complex in that it is necessary to ensure the forming quality of the inner ribs as well as the surface quality of the spun part. Spinning formability of thin-walled tubular parts with longitudinal inner ribs depends mainly on appropriate choosing of the process variables. However, there is no concrete objective function, so conventional optimization method cannot be used to optimize the process parameters so as to obtain the spun part with the desired inner ribs. The rapid development of back-propagation artificial neural network (BPANN) technology causes it to play a significant role in backward ball spinning of thin-walled tubular parts with longitudinal inner ribs.

As a nonlinear information processing system, BPANN is characterized by nonlinearity, adaptability, high parallelism, learning and generalization capabilities, and fault and failure tolerance (Basheer and Hajmeer, 2000). BPANN is also a relatively new computational tool that has found extensive utilization in solving many complex problems in plastic working domain (Kim and Kim, 2000; Ko et al., 1999), such as predicting flow stress (Wu et al., 2001), forecasting rolling force (Gunasekera et al., 1998), optimizing the irregular shape rolling process (Kim et al., 2001), predicting springback in metal forming (Inamdar et al., 2000), predicting fatigue life of carbon steel (Todd Pleune and Chopra, 2000), predicting fracture toughness in microalloy steel (Haque and Sudhakar, 2002).

In this paper, BPANN is first used in backward ball spinning of thin-walled tubular part with longitudinal inner ribs. BPANN is used for predicting the height of inner ribs as well as modeling the influences of the process parameters on the formability of inner ribs so that the process parameters can be matched rationally and the required spun parts can be obtained further.

2. Experimental

As shown in Fig. 1, in the course of backward ball spinning of thin-walled tubular part with longitudinal inner ribs, the spinning head, which consists of screw tube, supporting ring, conical ring and balls, is fixed in the chuck of the spinning machine and turns with the principal axis of the spinning machine, at the same time, the tubular blank made from 5A02 aluminum alloy is mounted on the mandrel and feeds with the mandrel along the axial direction. The mandrel has the grooves to form the inner ribs. The structure of the cross-section of the mandrel is shown in Fig. 2. The specific dimension of the cross-section is expressed as follows: $b = 3.5$ mm, $c = 2$ mm, $e = 2$ mm, $D = 30$ mm.

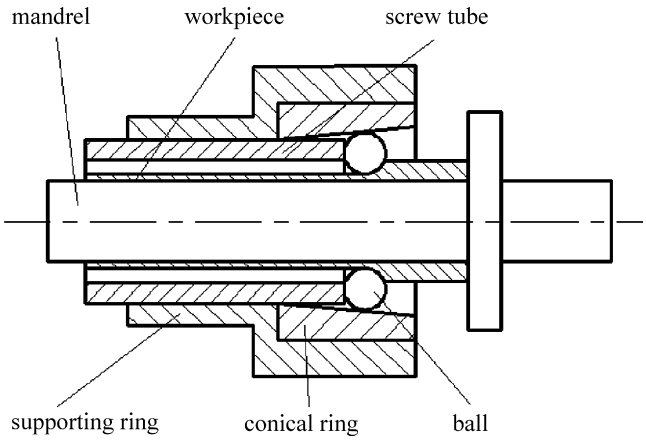

Fig. 1 – Schematic diagram of backward ball spinning.

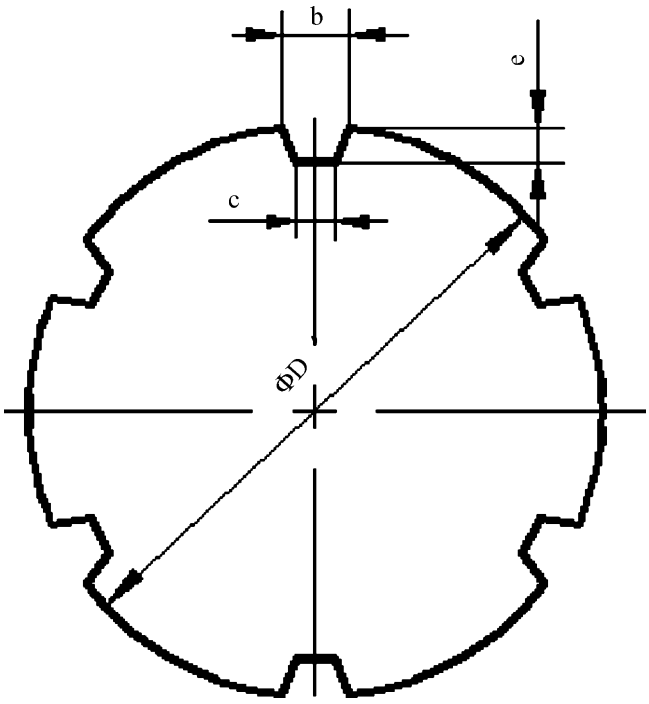

Fig. 2 – Schematic diagram of the cross-section of the mandrel.

Adjusting the relative displacement between supporting ring and screw tube results in the different gap between the balls and the mandrel, so the different wall thickness reduction is implemented so as to manufacture the spun parts with various wall thickness and diameter (as shown in Fig. 3).

3. Application of BPANN for predicting the fomability of the inner ribs

3.1. *Fundamentals of ANN*

3.1.1. *Artificial neuron model*

Artificial neuron (as shown in Fig. 4) is an information processing element that has many inputs but an output. If the neuron is the jth one, and the inputs which it receives from the other

Fig. 3 – Photograph of the spun part.

n neurons are x_1, x_2,..., x_n, respectively, and the connection weights between the jth neuron and the other n neurons are w_{1j}, w_{2j},..., w_{nj}, respectively.

$$y_j = f\left(\sum_{i=1}^{n} w_{ij}x_i - \theta_j\right) \quad (1)$$

where θ_j is the threshold of the neuron, y_j the output of the neuron, and f is the transfer function.

3.1.2. *Transfer function*

The transfer function is the basic Sigmoid, which possesses the distinctive properties of nonlinearity, continuity and differentiability on $(-\infty, +\infty)$. The sigmoid function is expressed as:

$$f(x) = \frac{1}{1+\exp(-x)} \quad (2)$$

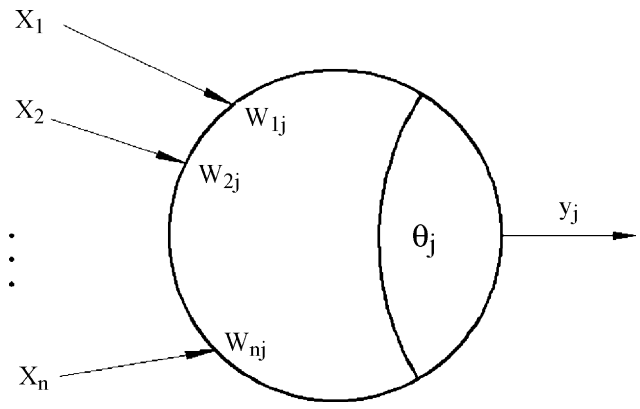

Fig. 4 – Schematic diagram of neuron model.

3.1.3. *Network structure*

Network structure is a three-layer feed forward network consisting of an input layer, a hidden layer and an output layer. In the network, the data are fed forward into the network without feedback, i.e., all links between neurons are unidirectional and there are no neuron-to-neuron connections in the same layer. Unlike the neurons of the input layer, the neurons of the hidden layer and output layer possess computational property.

3.1.4. *BP algorithm*

The back-propagation (BP) learning algorithm is based on searching an error surface using gradient descent for point with minimum error. The algorithm of training a BP network is summarized as follows:

(1) Initialize weights and thresholds, namely assign arbitrary small random values for the weights and thresholds.
(2) Present training data, i.e., present the input vectors and the desired outputs.
(3) Calculate the actual output y_j of the network.

$$y_j = f\left(\sum_i w_{ij}x_i - \theta_j\right) \quad (3)$$

where f is the sigmoid function.

(4) Calculate the error E of the network

$$E = \tfrac{1}{2}\sum_j (y_j - y_j^*)^2 \quad (4)$$

where the jth neuron is in the output layer, y_j the actual output and y_j^* is the target output. Assume ε is the allowable error accuracy, and if $\varepsilon < E$, then save initial weights and thresholds, and finish training, otherwise carry out the next step.

(5) Calculate all nodes error of the output layer and hidden layer.
If the jth neuron is in the output layer, δ_j is calculated from

$$\delta_j = y_j(1-y_j)(y_j - y_j^*) \quad (5)$$

If the jth neuron is in the hidden layer, δ_j is determined from

$$\delta_j = y_j(1-y_j)\sum_k \delta_k w_{jk} \quad (6)$$

(6) Adjust the weights and thresholds according to the error back-propagation direction.

$$w_{ij}^{(t+1)} = w_{ij}^{(t)} + \eta\delta_j y_i \quad (7)$$

$$\theta_j^{(t+1)} = \theta_j^{(t)} + \eta\delta_j \quad (8)$$

If a momentum coefficient is used, then

$$w_{ij}^{t+1} = w_{ij}^{t} + \eta\delta_j y_i + \alpha(w_{ij}^{t} - w_{ij}^{t-1}) \quad (9)$$

$$\theta_j^{t+1} = \theta_j^{t} + \eta\delta_j + \alpha[\theta_j^{t} - \theta_j^{t-1}] \quad (10)$$

where η is the learning rate, and α is the momentum coefficient.

(7) Return to (2) to compute repeatedly until the error agrees with the prespecified tolerance.

3.2. Critical issues in ANN

3.2.1. Network size

3.2.1.1. Network layer size. Too many hidden layers not only leads to slow learning, but results in overfitting and poor generalization of the network. A three-layer feed forward BP network can approximate any arbitrary continuous nonlinear function to any degree of accuracy, so a three-layer network including only one hidden layer is sufficient to meet the demand of the actual problem.

3.2.1.2. Input layer neuron size. The number of nodes in the input layer is determined according to the problem to be solved. According to the experimental situation, the height of inner ribs depends mainly on five variables, including spinning material, ball diameter, feed ratio, wall thickness reduction and wall thickness of tubular blank. However, in the experiment, the same spinning material is used and the wall thickness of the final spun products is identical, so the height of inner ribs depends mainly on ball diameter, feed ratio and wall thickness of tubular blank. As a result, the network chooses ball diameter, feed ratio and wall thickness of tubular blank as the input variables so that the number of nodes in the input layer can be 3.

3.2.1.3. Output layer neuron size. Because forming the desired height of inner ribs is one of the most critical tasks in backward ball spinning of thin-walled tubular part with longitudinal inner ribs, the height of inner ribs is selected the output variable of the network so as to determine the number of nodes in the output layer as 1.

3.2.1.4. Hidden layer neuron size. A network with too few hidden nodes is incapable of differentiating between complex patterns leading to only a linear estimate of the actual trend. In contrast, if the network has too many hidden nodes, it will follow the noise in the data due to overparameterization leading to poor generalization for untrained data. On the other hand, with increasing number of hidden nodes, training becomes excessively time-consuming. It is shown generally that when the number of nodes in the hidden layer is as two times or so as the number of nodes in the input layer, the network can be more compatible in terms of the capacity and training time. According to the rule, the number of nodes in the hidden layer is 8. Therefore, the structure of the network is as shown in Fig. 5 where X_1, X_2 and X_3 represent the ball diameter, the feed ratio and the wall thickness of tubular blank, respectively, and Y indicates the height of the inner ribs.

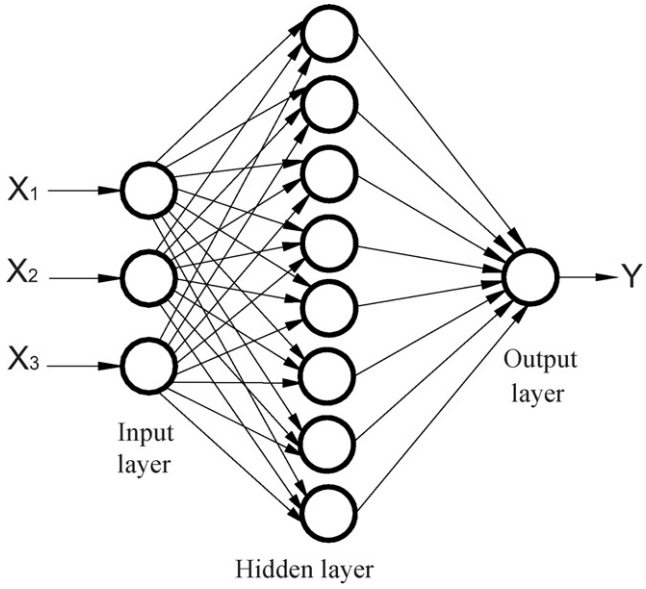

Fig. 5 – Schematic diagram of ANN structure.

3.2.2. Example data

The number of training example data has a great effect on computational property of the network. Data to be used for training BPANN should be large enough to cover the possible known variation in the problem domain. Too few example data lead to the instability of the computing result of the network. In contrast, too many example data result in no convergence as well as overfitting of the network. Currently, there are no mathematical rules for the determination of the required sizes of the example data. In the paper, the database derived from the experiment includes 60 example data, in which 40 example data are used to train the network to update the weights of the network, and 20 example data are used to check the response for untrained data and confirm the accuracy of the network.

3.2.3. Learning rate and momentum coefficient

A high learning rate will accelerate training by changing the weight vector. However, this may cause the search to oscillate on the error surface and never converge, thus increasing the risk of overshooting a near-optimal weight. In contrast, a small learning rate drives the search steadily in the direction of the global minimum, though slowly. To achieve an optimal weigh vector, it is necessary to use an adaptive learning rate $\eta(t)$, which varies along the course of training.

$$\text{If } E_{t+1} < E_t, \quad \text{then } \eta(t+1) = (1+\beta)\eta(t) \quad (11)$$

$$\text{If } E_{t+1} \geq E_t, \quad \text{then } \eta(t+1) = (1-\beta)\eta(t) \quad (12)$$

where E is the error, and β is a small positive number, generally $\beta = 0.01$–0.03.

A momentum coefficient is commonly used in weight updating to help the search escape local minima and reduce the likelihood of search instability. A high momentum coefficient will reduce the risks of the network being stuck in local minima, but it increases the risk of overshooting the solution

as does a high learning rate. Conversely, an extremely small momentum coefficient leads to slow training. It is suggested that momentum coefficient be between 0 and 1.

3.2.4. *Data normalization*

Normalization of data within a uniform range is essential to preventing larger numbers from overriding smaller ones and to preventing premature saturation of hidden nodes, which impedes the learning process. Input and output variables are normalized in interval (0, 1) corresponding to the range of the transfer function. However, in order to avoid saturation of the sigmoid function leading to slow or no learning between 0 and 0.1 as well as between 0.9 and 1, it is recommended that the data be normalized between 0.1 and 0.9. The normalization formula is as follows:

$$Z_n = 0.8\frac{Z - Z_{min}}{Z_{max} - Z_{min}} + 0.1 \quad (13)$$

where Z_n is the normalized value of Z, and Z_{max} and Z_{min} are the maximum and minimum values of Z in the database, respectively.

3.3. *ANN training*

The 40 representative training data is put into the network so as to lead to the convergence of the network (as shown in Fig. 6) and subsequently the 20 test data is put into the network in order to validate the accuracy of the network. The network trained satisfactorily is applied for predicting the 40 training data and the 20 test data and it is necessary to compare predicted values with experimental values (as shown in Fig. 7).

Seen from Fig. 7, as for 40 training data, the average relative error between the actual solution and the target solution is not more than 7%; as for 20 test data, the average relative error is not more than 8%. It is evident that the network is able to predict the height of inner ribs reasonably well.

3.4. *ANN modeling*

The input layer of the BPANN contains the three independent variables, namely ball diameter, feed ratio and wall thickness of tubular blank, and the node of the output layer is the height of inner ribs. The network can, respectively, model the influences of the three variables on the height of inner ribs. One way is that when mimicking the influence of one variable, the variable varies but the other two variables take constant values. According to the method, a sample of simulation curves in comparison with their experimental counterparts is obtained in Figs. 8–10. It is obvious that the simulated results agree well with the experimental counterparts.

Fig. 8 shows the curve of the height of the inner ribs with respect to the diameter of ball under the tubular blank with the wall thickness of 3.0 mm and the feed ratio with 1.0 mm/r. It is seen from Fig. 7 that increasing the ball diameter can increase the height of the inner ribs, and at the early stage, the height of the inner ribs grows sharply, but when the diameter of the ball reaches a certain value, the height of the inner ribs increases slowly. Increasing the ball size leads to the increase of the spin-

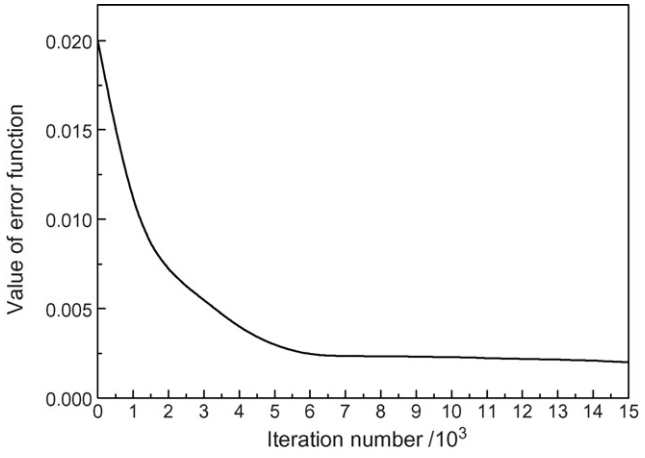

Fig. 6 – Schematic diagram of network convergence.

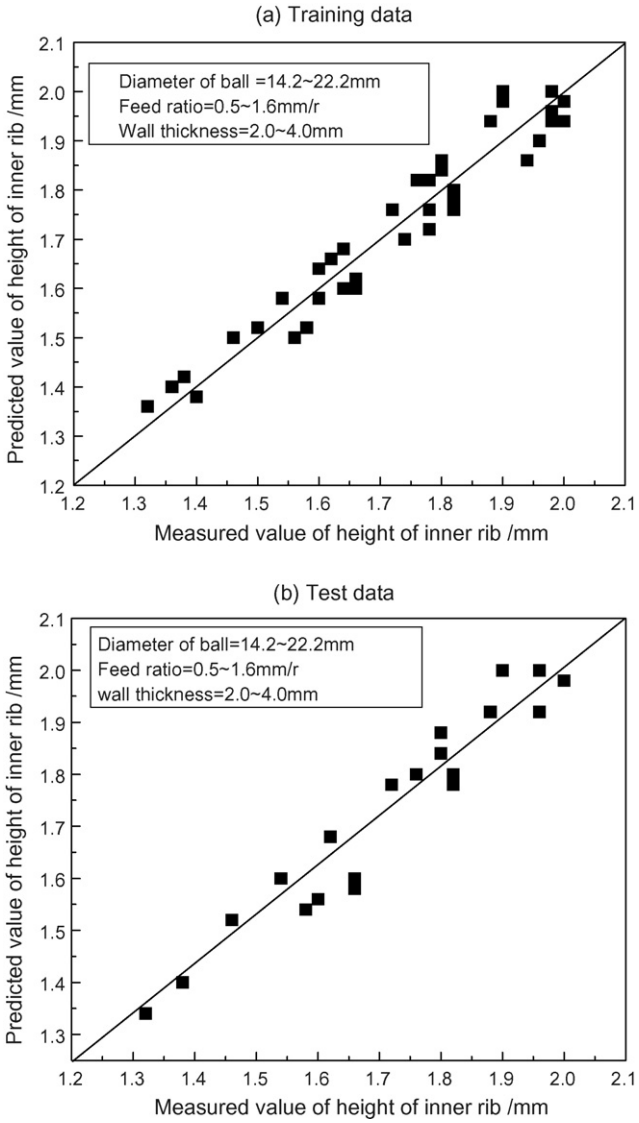

Fig. 7 – Contrast between predicted values and measured with respect to the height of inner rib: (a) training data and (b) test data.

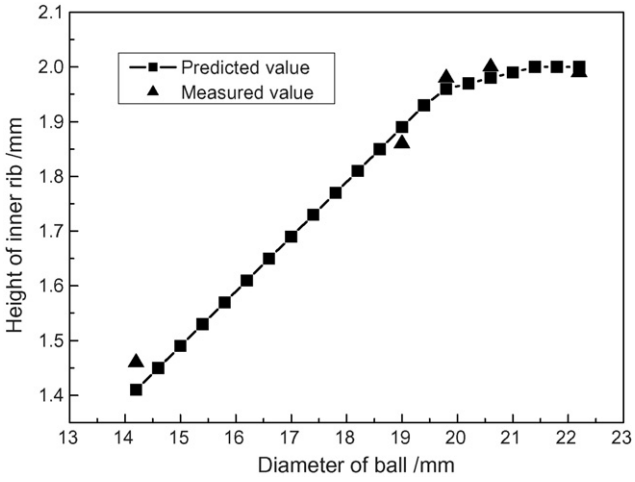

Fig. 8 – The curve of height of inner rib with respect to diameter of ball.

ning force as well as the stable flow of the metal material, which contributes greatly to the forming of the inner ribs.

Fig. 9 shows the curve of the height of the inner ribs with respect to the wall thickness of tubular blank under the ball with the diameter of 20 mm and the feed ratio with 1.0 mm/r. It is seen from Fig. 9 that there exists a extremum point to result in the highest inner ribs at the curve, i.e., before the extremum point, the height of inner ribs increases with the increase of wall thickness of tubular blank, and after the extremum point, the height of inner ribs decreases with the increase of wall thickness of tubular blank. The reason for the above phenomenon is that the thicker tubular blank needs the more spinning passes to lead to the working hardening of the metal material, which has an adverse influence on the formability of the inner ribs.

Fig. 10 shows the curve of the height of the inner ribs with respect to the feed ratio under the tubular blank with the wall thickness of 3.0 mm and the ball with the diameter of 20 mm.

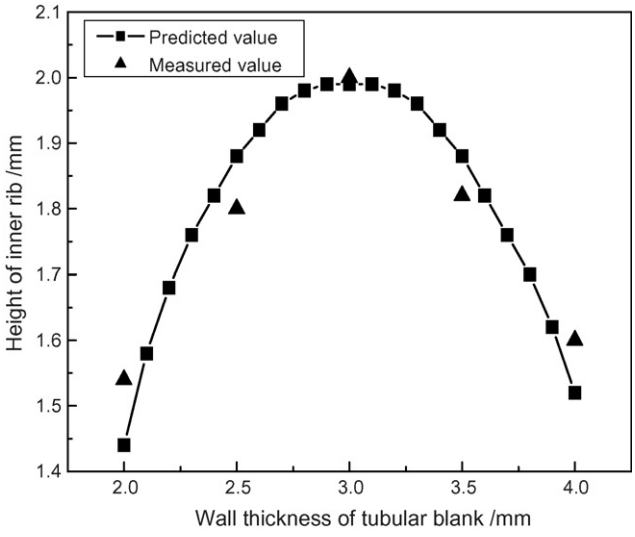

Fig. 9 – The curve of height of inner rib with respect to wall thickness of tubular blank.

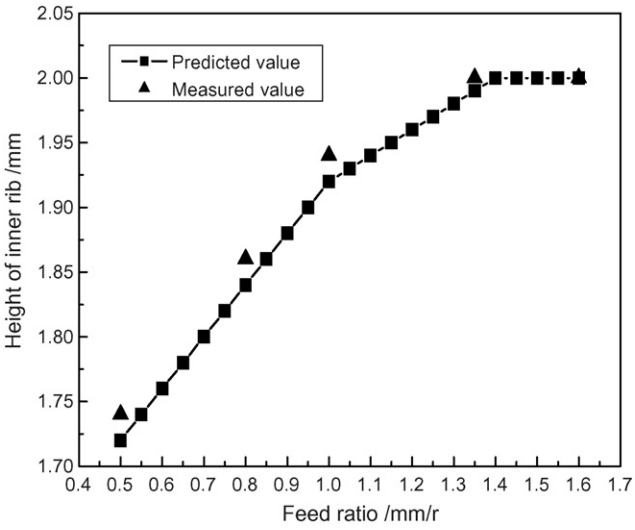

Fig. 10 – The curve of height of inner rib with respect to feed ratio.

Seen from Fig. 10, the height of the inner ribs increases with the increase of the feed ratio, and at the early stage, the height of the inner ribs grows sharply, but when the feed ratio reaches a certain value, the height of the inner ribs increases slowly. Increasing the feed ratio is capable of increasing the spinning force as well as enhancing the formability of the inner ribs, but too large a feed ratio leads to the poor surface finish of the spun part.

4. Conclusions

(1) Obtaining the desired inner ribs is one of the most critical tasks in backward ball spinning of thin-walled tubular part with longitudinal inner ribs and the formability of the inner ribs depends mainly on ball diameter, feed ratio, and wall thickness of tubular blank. BPANN can accurately predict the formability of the inner ribs as well as simulating the influences of process parameters, such as ball diameter, feed ratio, and wall thickness of tubular blank on the formability of the inner ribs. In general, the height of the inner ribs increases with increasing the ball diameter as well as the feed ratio. With a view to forming a certain high inner rib on the condition that the other process parameters take constant values, there exists the best wall thickness value.

(2) The design of BPANN structure mainly deals with the selection of the transfer function and the determination of the network parameters, such as network layer size, all layers neurons size, learning rate and momentum factor. At the same time, the normalization formula, the initialization of weights and threshold, and the example data size have a significant influence on the properties of the network. In order to make the BPANN show stronger prediction and simulation capabilities, the optimization of the network parameters is essential to develop the BPANN.

(3) Though a three-layer BPANN shows a large superiority in predicting and simulating the spinning process, it should

be recognized that BPANN has many limitations that should not be overlooked. For instance, the prediction and simulation accuracy depends greatly on the quantity and quality of the BPANN. On the other hand, there is no explicit mathematics rule in the determination of the number of the hidden neurons, so the BPANN will need to be perfected further in the future.

REFERENCES

Basheer, I.A., Hajmeer, M., 2000. Artificial neural networks: fundamentals, computing, design, and application. J. Microbiol. Methods 43, 3–31.

Chang, S.C., Huang, C.A., Yu, S.Y., et al., 1998. Tube spinnability of AA 2024 and 7075 aluminum alloys. J. Mater. Process. Technol. 80/81, 676–682.

Gunasekera, J.S., Zhengjie, Jia, Malas, J.C., et al., 1998. Development of a neural network model for a cold rolling process. Eng. Appl. Artif. Intell. 11, 597–603.

Haque, M.E., Sudhakar, K.V., 2002. ANN back-propagation prediction model for fracture toughness in microalloy steel. Int. J. Fatigue 24, 1003–1010.

Inamdar, M.V., Date, P.P., Desai, U.B., 2000. Studies on the prediction of springback in air vee bending of metallic sheets using an artificial neural network. J. Mater. Process. Technol. 108, 45–54.

Jiang, S.Y., Xue, K.M., Zong, Y.Y., et al., 2004. Process factors influencing spinning deformation of thin-walled tubular part with longitudinal inner ribs. Trans. Nonferrous Met. Soc. China 14, 702–707.

Jiang, S.Y., Xue, K.M., Li, C.F., et al., 2006. Spinning deformation criteria of thin-walled tubular part with longitudinal inner ribs. J. Wuhan Univ. Technol.-Mater. Sci. Ed. 21, 169–172.

Kim, D.J., Kim, B.M., 2000. Application of neural network and FEM for metal forming processes. Int. J. Mach. Tools Manuf. 40, 911–925.

Kim, D.J., Kim, Y.C., Kim, B.M., 2001. Optimization of the irregular shape rolling process with an artificial neural network. J. Mater. Process. Technol. 113, 131–135.

Ko, Dae-Cheol, Kim, Dong-Hwan, Kim, Byung-Min, 1999. Application of artificial neural network and Taguchi method to preform design in metal forming considering workability. Int. J. Mach. Tools Manuf. 39, 771–785.

Rotarescu, M.I., 1995. A theoretical analysis of tube spinning using balls. J. Mater. Process. Technol. 54, 224–229.

Todd Pleune, T., Chopra, K.O., 2000. Using artificial neural networks to predict the fatigue life of carbon and low-alloy steels. Nucl. Eng. Des. 197, 1–12.

Wong, C.C., Dean, T.A., Lin, J., 2003. A review of spinning, shear forming and flow forming process. Int. J. Mach. Tools Manuf. 43, 1419–1435.

Wu, R.H., Liu, H.B., Chang, H.B., Hsu, T.Y., Ruan, X.Y., 2001. Prediction of the flow stress of 0.4C–1.9Mn–1.0Ni–0.2Mo steel during hot deformation. J. Mater. Process. Technol. 116, 211–218.

Xue, K.M., Lu, Y., 1997. A study of the rational matching relationships amongst technical parameters in stagger spinning. J. Mater. Process. Technol. 69, 167–171.